Journal of Medical Sciences

ISSN 1682-4474

science alert

ANSInet
an open access publisher
http://ansinet.com

Research Paper

J. Med. Sci., 6 (2): 262-274
March-April, 2006

Discrete Cosine Transform Based Gradient Vector Flow Active Contours-A Suitable Tool for Chromosome Image Classification

[1]A. Prabhu Britto and [2]G. Ravindran

In this study, the suitability of the Discrete Cosine Transform (DCT) based Gradient Vector Flow (GVF) Active Contour as a suitable tool for Chromosome image classification is assessed. The DCT based GVF active contour has been established as an efficient tool for chromosome image segmentation in chromosome spread images. From the performance of DCT based GVF active contour in chromosome segmentation, insight has been obtained that recommends the same technique as a chromosome image classification tool. This study discusses and establishes that DCT based GVF active contour can be used as a suitable tool for chromosome image classification.

Key words: Gradient vector flow, active contour, discrete cosine transform, chromosome, classification

JMS (ISSN 1682-4474) is an International, peer-reviewed scientific journal that publishes original article in experimental & clinical medicine and related disciplines such as molecular biology, biochemistry, genetics, biophysics, bio-and medical technology. JMS is issued six times per year on paper and in electronic format.

For further information about this article or if you need reprints, please contact:

A. Prabhu Britto
Center for Medical Electronics,
Department of Electronics and Communication Engineering,
Anna University, Chennai,
600025, India

ANSInet
Asian Network for Scientific Information

[1]Center for Medical Electronics, Department of Electronics and Communication Engineering,
[2]Faculty of Information and Communication Engineering, Anna University Chennai 600025, India

INTRODUCTION

Gradient Vector Flow (GVF) active contours have been used for successful segmentation of chromosome spread images (Britto and Ravindran, 2005). This research work used a variant of Gradient vector flow active contour, called Discrete Cosine Transform (DCT) based Gradient Vector Flow (GVF) active contour which has been established as a better segmentation tool for chromosome spread images, compared to GVF Active contours and its variants (Britto and Ravindran, 2005). The DCT based GVF active contour has hence been characterized (Britto and Ravindran, 2005) and standardized (Britto and Ravindran, 2005) for segmenting chromosome images from chromosome spread images. The segmentation has been accurately done establishing that DCT based GVF active contours are an efficient tool for chromosome image segmentation. From the segmentation results, further insight has been obtained that substantiates that DCT based GVF Active Contours can also be used for classification of chromosome images. This paper discusses analytically, the suitability of DCT based GVF active contours as a tool for chromosome image classification.

Chromosome images: A chromosome is an extended DNA molecule containing multiple genes and associated proteins. During mitosis and meiosis, condensed chromosomes form structures that are visible with high-powered light microscopes (<http://www.colorado .edu/MCDB/MCDB2150Fall/notes00/L0001.html>). The chromosome spread images are obtained using the following general procedure. About 5 mL of blood is removed from the patient. If a fetus is being karyotyped, amniotic fluid is removed from the amniotic sac which surrounds the fetus during development. This is done with the aid of a large syringe and ultrasound picturing. There are cells which have come off the fetus in this fluid. The white blood cells are removed from the blood or the living cells are removed from the amniotic fluid. These cells are then cultured in a medium in which they undergo mitosis. Mitosis is stopped at metaphase using chemicals. The cells are then placed onto a slide spread out. They are viewed under a microscope which is specially adapted with a camera to take a picture of the chromosomes from one of the cells (<http://home.earthlink.net/~heinabilene /karyotypes/karyoty.htm>).

Hence, the chromosomes in a spread image have variations in shape caused due to bending effects, variations due to overlaps, variations due to illumination and device dependencies. This causes difficulties in segmenting the chromosome images as the segmenting algorithm or technique needs to be retrained often. Therefore, gradient vector flow active contour, a special class of deformable curves is chosen to perform good and efficient segmentation of chromosome spread images under such difficulties caused by so much of variation.

Chromosome structure and classification: The human chromosome consists of 22 pairs of autosomes and one pair of sex chromosomes (X and Y chromosome). Each pair of the autosomes and each of the sex chromosomes vary from each other and the absolute length of any chromosome varies depending on the stage of mitosis in which it was fixed (Fig. 1). However, the relative position of the centromere is constant, which means that the ratio of the lengths of the two arms is constant for each chromosome. This ratio is an important parameter for chromosome classification (<http://arbl.cvmbs. colostate.edu/hbooks/genetics/medgen/chromo/chromo somes.html>).

Chromosomes are arranged into seven groups based on size and centromere location. The centromeres can be found in the middle of the chromosome (median), near one end (acrocentric), or in between these first two (submedian) (<http://home.earthlink.net/~heinabilene /karyotypes/karyoty.htm>)

- Group A: Chromosomes 1-3 are largest with median centromere.
- Group B: Chromosomes 4-5 are large with submedian centromere
- Group C: Chromosomes 6-12 are medium sized with submedian centromere
- Group D: Chromosomes 13-15 are medium sized with acrocentric centromere
- Group E: Chromosomes 16-18 are short with median or submedian centromere
- Group F: Chromosomes 19-20 are short with median centromere
- Group G: Chromosomes 21-22 are very short with acrocentric centromere.

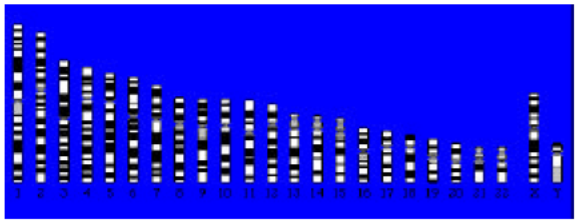

Fig. 1: Idiogram of human chromosomes (<http://home.earthlink.net/~heinabilene/karyotypes/karyoty.htm>)

- Chromosome X is similar to Group C.
- Chromosome Y is similar to Group G

DCT based GVF active contours have been used to successfully segment chromosome images. The segmentation observations indicate that DCT based GVF active contours can also be used for chromosome image classification.

Gradient Vector Flow (GVF) active contours: Gradient Vector Flow (GVF) Active Contours use Gradient Vector Flow fields obtained by solving a vector diffusion equation that diffuses the gradient vectors of a gray-level edge map computed from the image. The GVF active contour model cannot be written as the negative gradient of a potential function. Hence it is directly specified from a dynamic force equation, instead of the standard energy minimization network.

The external forces arising out of GVF fields are non-conservative forces as they cannot be written as gradients of scalar potential functions. The usage of non-conservative forces as external forces show improved performance of gradient vector flow field active contours compared to traditional energy minimizing active contours (Xu and Prince, 2000; Xu and Prince, 1998).

The GVF field points towards the object boundary when very near to the boundary, but varies smoothly over homogeneous image regions extending to the image border. Hence the GVF field can capture an active contour from long range from either side of the object boundary and can force it into the object boundary. The GVF active contour model thus has a large capture range and is insensitive to the initialization of the contour. Hence the contour initialization is flexible.

The gradient vectors are normal to the boundary surface but by combining laplacian and gradient the result is not the normal vectors to the boundary surface. As a result of this, the GVF field yields vectors that point into boundary concavities so that the active contour is driven through the concavities. Information regarding whether the initial contour should expand or contract need not be given to the GVF active contour model. The GVF is very useful when there are boundary gaps, because it preserves the perceptual edge property of active contours (Xu and Prince, 1998; Kass *et al*., 1987).

The GVF field is defined as the equilibrium solution to the following vector diffusion equation (Xu and Prince, 2000),

$$u_t = g(|\nabla f|)\nabla^2 u - h(|\nabla f|)(u - \nabla f) \quad (1a)$$

$$u(x,0) = \nabla f(x) \quad (1b)$$

Where, u_t denotes the partial derivative of u(x,t) with respect to t, ∇^2 is the Laplacian operator (applied to each spatial component of u separately) and f is an edge map that has a higher value at the desired object boundary.

The functions in g and h control the amount of diffusion in GVF. In Eq. 1, $g(|\nabla f|)\nabla^2$ produces a smoothly varying vector field and hence called as the smoothing term, while $h(|\nabla f|)$ $(u-\nabla f)$ encourages the vector field u to be close to ∇f computed from the image data and hence called as the data term. The weighting functions $g(\cdot)$ and $h(\cdot)$ apply to the smoothing and data terms respectively and they are chosen (Xu and Prince, 1998) as $g(|\nabla f|) = \mu$ and $h(|\nabla f|) = |\nabla f|^2$. $g(\cdot)$ is constant here and smoothing occurs everywhere, while $h(\cdot)$ grows larger near strong edges and dominates at boundaries.

Hence, the Gradient Vector Flow field is defined as the vector field v(x,y)=[u(x,y),v(x,y)] that minimizes the energy functional

$$\varepsilon = \iint \mu(u_x^2 + u_y^2 + v_x^2 + v_y^2) + |\nabla f|^2 |v - \nabla f|^2 \, dxdy \quad (2)$$

The effect of this variational formulation is that the result is made smooth when there is no data.

When the gradient of the edge map is large, it keeps the external field nearly equal to the gradient, but keeps field to be slowly varying in homogeneous regions where the gradient of the edge map is small, i.e., the gradient of an edge map ∇f has vectors point toward the edges, which are normal to the edges at the edges and have magnitudes only in the immediate vicinity of the edges and in homogeneous regions ∇f is nearly zero. μ is a regularization parameter that governs the tradeoff between the first and the second term in the integrand in Eq. 2. The solution of Eq. 2 can be done using the Calculus of Variations and further by treating u and v as functions of time, solving them as generalized diffusion equations (Xu and Prince, 2000).

Discrete Cosine Transform (DCT) based GVF active contours: The transform of an Image yields more insight into the properties of the image. The Discrete Cosine Transform has excellent energy compaction. Hence, the Discrete Cosine Transform promises better description of the image properties. The Discrete Cosine Transform is embedded into the GVF Active Contours. When the image property description is significantly low, this helps the contour model to give significantly better performance by utilizing the energy compaction property of the DCT.

The 2D DCT is defined as:

$$C(u,v) = a(u)a(v)\sum_{x=0}^{N-1}\sum_{y=0}^{N-1} f(x,y) \cos\left[\frac{(2x+1)u\pi}{2N}\right]\cos\left[\frac{(2x+1)v\pi}{2N}\right] \quad (3)$$

The local contrast of the Image at the given pixel location (k,l) is given by

$$P(k,l) = \frac{\sum^{2(2n+1)-1} w_t E_t}{d_{00}} \quad (4)$$

where,

$$E_t = \frac{\sum_{u+v=t} |d_{u,v}|}{N} \quad (5)$$

and

$$N = \begin{cases} t+1 & t<2n+1 \\ 2(2n+1)-t & t \geq 2n+1 \end{cases} \quad (6)$$

Here, w_t denotes the weights used to select the DCT coefficients. The local contrast P(k,l) is then used to generate a DCT contrast enhanced Image (Tang and Acton, 2004), which is then subject to selective segmentation by the energy compact gradient vector flow active contour model using Eq. 2.

MATERIALS AND METHODS

The chromosome metaphase image (at 72 ppi resolution) provided by Prof. Ken Castleman and Prof.Qiang Wu (Advanced Digital Imaging Research, Texas) was taken and preprocessed. Insignificant and unnecessary regions in the image were removed interactively.

Interactive selection of the chromosome of interest was done by selecting a few points around the chromosome that formed the vertices of a polygon. On constructing the perimeter of the polygon, seed points for the initial contour were determined automatically by periodically selecting every third pixel along the perimeter of the polygon.

The GVF deformable curve was then allowed to deform until it converged to the chromosome boundary. The optimum parameters for the deformable curve with respect to the Chromosome images were determined by tabulated studies.

The image was made to undergo minimal preprocessing so as to achieve the goal of boundary mapping in chromosome images with very weak edges.

The DCT based GVF Active contour is governed by the following parameters, namely, σ, μ, α, β and κ. σ determines the Gaussian filtering that is applied to the image to generate the external field.

Larger value of σ will cause the boundaries to become blurry and distorted and can also cause a shift in the boundary location. However, large values of σ are necessary to increase the capture range of the active contour. μ is a regularization parameter in Eq. 2 and requires a higher value in the presence of noise in the image. α determines the tension of the active contour and β determines the rigidity of the contour. The tension keeps the active contour contracted and the rigidity keeps it smooth. α and β may also take on value zero implying that the influence of the respective tension and rigidity terms in the diffusion equation is low. κ is the external force weight that determines the strength of the external field that is applied. The iterations were set suitably.

RESULTS AND DISCUSSION

Characterization of parameters of the DCT based GVF active contour segmentation scheme has yielded the values of $\sigma = 0.25$, $\mu = 0.075$, $\alpha = 0$, $\beta = 0$ and $\kappa = 0.625$ as characterized parameter values (Britto and Ravindran, 2005). Standardization experiments have established that the characterized parameter values are indeed standardized and can be used for segmenting chromosome spread images from any dataset (Britto and Ravindran, 2005). Therefore, chromosome images from three independent datasets.

Three hundred and eighteen images from three datasets were segmented using DCT based GVF active contours. A sample image, its DCT based GVF field and its corresponding segmented image are shown below (Fig. 2a-c).

Chromosome images were drawn from three independent datasets and subjected to segmentation. A few segmented chromosome image samples are shown below (Fig. 3-42).

Studies on the 318 chromosome images used for segmentation and their corresponding segmented output images revealed the following observations (Table 1).

Though visual inspection by the naked eye does not find errors, from the table above, it is found that there is a very small segmentation error. The ratio of the lengths (major axis diameter) of the original chromosome image to the boundary mapped chromosome image reveals that the ratio is almost constant with a standard deviation of only 0.02 or 2%. Similarly, the ratio of the areas has a standard deviation of only 0.04 or 4%. Hence, the length or area

Fig. 2a: Sample chromosome image

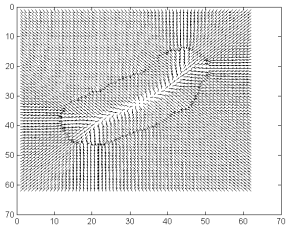

Fig.2b: DCT based GVF field of Fig.1a

Fig.2c: Segmented output image of Fig.1a

Fig. 3: Segmented sample 1

Fig. 4: Segmented sample 2

Fig. 5: Segmented sample 3

Fig. 6: Segmented sample 4

Fig.7: Segmented sample 5

Fig. 8: Segmented sample 6

Fig. 9: Segmented sample 7

Fig. 10: Segmented sample 8

Fig. 11: Segmented sample 9

Fig. 12: Segmented sample 10

Fig. 13: Segmented sample 11

Fig.14: Segmented sample 12

Fig. 15: Segmented sample 13

Fig. 16: Segmented sample 14

Fig.17: Segmented sample15

Fig. 18: Segmented sample 16

Fig. 19: Segmented sample 17

Fig. 20: Segmented sample 18

Fig. 21: Segmented sample 19

Fig. 22: Segmented sample 20

Fig. 23: Segmented sample 21

Fig. 24: Segmented sample 22

Fig. 25: Segmented sample 23

Fig. 26: Segmented sample 24

Fig. 27: Segmented sample 25

Fig. 28: Segmented sample 26

Fig. 29 Segmented sample 27

Fig. 30: Segmented sample 28

Fig. 31: Segmented sample 29

Fig. 32: Segmented sample 30

Fig.33: Segmented sample 31

Fig. 34: Segmented sample 32

Fig.35: Segmented sample 33

Fig. 36: Segmented sample 34

Fig. 37: Segmented sample 35

Fig. 38: Segmented sample 36

Fig. 39: Segmented sample 37

Fig. 40: Segmented sample 38

Fig. 41: Segmented sample 39

Fig. 42: Segmented sample 40

Table 1: Segmentation observations

No.	Boundary mapped image centroid	Original image major axis diameter (pixels)	Boundary mapped image major axis diameter (pixels)	Ratio (original dia./ boundary dia)	Original image area (square pixels)	Boundary mapped image area (square pixels)	Ratio (original area/ boundary mapped image area)
1	[26.9499 25.6187]	31.34	33.33	0.94	391	459	0.85
2	[37.4137 35.5959]	55.07	56.91	0.97	771	933	0.83
3	[30.5523 33.7788]	42.71	45.15	0.95	608	746	0.82
4	[34.5700 33.7837]	44.98	45.98	0.98	656	786	0.83
5	[35.2648 35.4926]	61.67	63.26	0.97	911	1080	0.84
6	[36.4190 35.2034]	53.06	55.50	0.96	816	988	0.83
7	[30.2827 31.8242]	40.84	44.05	0.93	582	711	0.82
8	[36.1808 36.1206]	57.86	60.07	0.96	830	1012	0.82
9	[28.0188 26.9401]	34.72	37.42	0.93	456	584	0.78
10	[24.6053 25.2177]	29.18	31.66	0.92	314	418	0.75
11	[29.4542 31.5989]	43.06	44.07	0.98	583	698	0.84
12	[26.2148 28.2852]	37.03	38.96	0.95	410	526	0.78
13	[31.6006 31.0858]	43.96	45.44	0.97	595	711	0.84
14	[27.4309 27.4839]	38.79	41.01	0.95	492	622	0.79
15	[23.2127 23.2689]	26.57	29.66	0.90	314	409	0.77
16	[27.2938 25.9799]	31.52	33.67	0.94	401	497	0.81
17	[30.4387 31.9555]	40.77	43.14	0.95	523	652	0.80
18	[34.4773 34.9714]	58.03	59.49	0.98	674	838	0.80
19	[28.2182 28.5818]	40.66	42.41	0.96	509	605	0.84
20	[42.4133 41.0889]	76.79	78.77	0.97	1128	1372	0.82
21	[29.9879 29.8956]	41.19	43.93	0.94	522	661	0.79
22	[34.4763 34.1872]	56.03	58.38	0.96	765	951	0.80
23	[38.0851 37.7864]	70.12	72.42	0.97	996	1222	0.82
24	[28.0394 27.0059]	34.58	36.74	0.94	421	507	0.83
25	[32.4387 32.5098]	44.04	44.92	0.98	552	661	0.84
26	[35.2357 36.8037]	59.57	61.36	0.97	859	1014	0.85
27	[36.3105 37.8500]	66.59	68.27	0.98	950	1140	0.83
28	[33.3139 31.9770]	49.46	51.84	0.95	684	825	0.83
29	[23.0113 23.4437]	30.71	32.54	0.94	363	444	0.82
30	[25.3586 24.8156]	31.60	33.99	0.93	390	488	0.80
31	[27.4389 29.0568]	38.24	40.40	0.95	459	581	0.79
32	[50.8241 50.7967]	101.06	103.67	0.97	1417	1717	0.83
33	[33.9449 33.9786]	57.35	59.44	0.96	802	980	0.82
34	[27.8979 28.1691]	36.98	39.13	0.94	511	627	0.81
35	[27.0169 26.8390]	30.74	33.13	0.93	370	472	0.78
36	[32.2975 30.3386]	44.01	44.40	0.99	556	632	0.88
37	[34.9535 34.0332]	45.71	47.72	0.96	623	752	0.83
38	[29.8076 31.8124]	36.59	39.13	0.94	514	629	0.82
39	[34.8909 33.8749]	55.92	58.30	0.96	693	871	0.80
40	[27.6118 29.6000]	37.71	40.85	0.92	468	595	0.79
41	[35.7299 32.0613]	45.40	45.53	1.00	582	685	0.85
42	[23.5082 23.7500]	24.59	27.41	0.90	258	364	0.71
43	[22.5170 23.9690]	22.98	24.90	0.92	247	323	0.76
44	[28.7891 29.8908]	36.86	39.15	0.94	400	531	0.75

Table 1: Continue

No.	Boundary mapped image centroid	Original image major axis diameter (pixels)	Boundary mapped image major axis diameter (pixels)	Ratio (original dia./ boundary dia)	Original image area (square pixels)	Boundary mapped image area (square pixels)	Ratio (original area/ boundary mapped image area)
45	[22.6156 24.8602]	25.94	28.24	0.92	297	372	0.80
46	[24.9346 25.6877]	28.56	31.46	0.91	327	413	0.79
47	[28.9533 30.6822]	38.91	40.38	0.96	439	535	0.82
48	[31.1326 31.8387]	41.25	42.76	0.96	533	626	0.85
49	[34.3674 34.2818]	49.87	51.53	0.97	710	841	0.84
50	[28.5336 29.6911]	40.75	43.64	0.93	532	654	0.81
51	[29.0348 29.5357]	38.77	39.64	0.98	505	575	0.88
52	[27.5009 30.1377]	38.66	41.02	0.94	493	581	0.85
53	[35.2575 35.9663]	52.87	55.07	0.96	674	800	0.84
54	[24.0698 24.1333]	24.20	25.90	0.93	254	315	0.81
55	[27.4715 27.9065]	33.27	34.97	0.95	413	492	0.84
56	[27.3134 28.4254]	29.50	32.35	0.91	290	402	0.72
57	[32.7654 33.6319]	53.29	55.46	0.96	741	891	0.83
58	[47.9236 48.9378]	93.42	95.43	0.98	1360	1624	0.84
59	[24.5156 26.0406]	23.61	25.89	0.91	234	320	0.73
60	[25.6719 25.7236]	29.58	31.69	0.93	348	445	0.78
61	[27.4764 27.3270]	32.11	34.20	0.94	418	529	0.79
62	[27.4000 29.3881]	32.76	35.26	0.93	402	505	0.80
63	[32.9788 35.6068]	49.76	52.25	0.95	602	707	0.85
64	[33.0557 34.2227]	47.89	50.08	0.96	747	880	0.85
65	[26.7024 27.0590]	24.32	27.28	0.89	295	373	0.79
66	[40.3481 40.6745]	58.53	61.83	0.95	887	1063	0.83
67	[26.5828 28.1795]	29.27	31.97	0.92	326	429	0.76
68	[40.4265 41.3790]	82.76	85.83	0.96	972	1198	0.81
69	[35.1370 37.6489]	61.81	63.45	0.97	728	883	0.82
70	[37.4309 38.0644]	60.97	64.02	0.95	666	854	0.78
71	[53.0434 55.5284]	106.01	108.24	0.98	1181	1427	0.83
72	[31.3701 30.8464]	47.83	50.18	0.95	596	716	0.83
73	[33.7503 35.5857]	51.98	54.87	0.95	577	741	0.78
74	[27.9612 27.0583]	30.40	33.20	0.92	409	515	0.79
75	[34.9546 37.2347]	55.30	57.61	0.96	819	1014	0.81
76	[29.8066 28.5959]	36.50	39.85	0.92	477	641	0.74
77	[35.1434 36.3841]	54.56	56.18	0.97	847	1018	0.83
78	[41.8959 39.5171]	63.30	65.41	0.97	1049	1230	0.85
79	[38.3850 42.6994]	66.08	69.01	0.96	1081	1304	0.83
80	[41.9167 42.1767]	75.73	77.59	0.98	1257	1500	0.84
81	[40.3016 39.8470]	70.62	72.97	0.97	1157	1366	0.85
82	[34.4716 33.9521]	54.30	56.93	0.95	793	1003	0.79
83	[35.1834 35.7918]	62.17	64.73	0.96	939	1172	0.80
84	[34.8285 37.4745]	60.55	63.96	0.95	938	1178	0.80
85	[40.8476 43.5766]	77.44	79.70	0.97	1208	1476	0.82
86	[42.4705 43.2510]	76.35	78.96	0.97	1222	1494	0.82
87	[30.3358 31.2473]	44.35	47.72	0.93	643	825	0.78
88	[29.1239 33.3478]	50.61	53.71	0.94	709	920	0.77
89	[23.7570 25.2645]	26.78	30.35	0.88	344	465	0.74
90	[34.7059 34.5823]	55.40	58.40	0.95	832	1027	0.81
91	[28.9291 28.6411]	37.35	40.85	0.91	518	677	0.77
92	[24.2281 24.5614]	30.40	33.83	0.90	389	513	0.76
93	[27.1866 28.7289]	36.32	38.90	0.93	433	568	0.76
94	[27.8122 27.8048]	35.65	37.88	0.94	426	543	0.78
95	[32.0986 33.1862]	40.79	43.12	0.95	545	639	0.85
96	[25.0922 27.3686]	32.11	32.81	0.98	433	510	0.85
97	[37.4195 38.9720]	56.83	60.15	0.94	719	894	0.80
98	[37.8234 39.8945]	52.56	55.21	0.95	708	872	0.81
99	[32.7925 32.6783]	49.71	51.39	0.97	659	805	0.82
100	[36.3938 36.3571]	54.11	57.04	0.95	696	871	0.80
101	[22.3883 23.8934]	24.99	27.69	0.90	296	394	0.75
102	[38.2407 35.6866]	51.40	52.95	0.97	956	1155	0.83
103	[31.8058 31.3716]	43.22	45.07	0.96	510	654	0.78
104	[29.8752 32.4832]	43.40	45.06	0.96	482	625	0.77
105	[39.2162 38.9653]	58.48	60.66	0.96	1109	1355	0.82
106	[34.0935 34.8745]	51.84	55.26	0.94	630	781	0.81
107	[34.5247 34.2760]	49.54	50.85	0.97	648	768	0.84
108	[27.7755 28.3750]	33.56	35.55	0.94	327	432	0.76

Table 1: Continue

No.	Boundary mapped image centroid	Original image major axis diameter (pixels)	Boundary mapped image major axis diameter (pixels)	Ratio (original dia./ boundary dia)	Original image area (square pixels)	Boundary mapped image area (square pixels)	Ratio (original area/ boundary mapped image area)
109	[29.4458 28.7311]	33.83	36.94	0.92	309	424	0.73
110	[30.7336 31.9097]	41.01	43.52	0.94	499	642	0.78
111	[28.6695 29.4762]	40.81	43.61	0.94	563	714	0.79
112	[43.2667 43.4667]	76.11	78.79	0.97	890	1125	0.79
113	[42.9310 43.5067]	79.16	81.52	0.97	1040	1275	0.82
114	[27.1307 27.2015]	35.57	38.50	0.92	403	551	0.73
115	[31.7546 31.6515]	49.79	53.47	0.93	653	815	0.80
116	[32.3812 33.7535]	44.97	48.07	0.94	615	787	0.78
117	[25.8393 26.6190]	31.00	33.16	0.93	381	504	0.76
118	[27.4894 27.0123]	32.91	35.00	0.94	462	568	0.81
119	[31.6831 31.1670]	48.37	50.00	0.97	707	874	0.81
120	[33.3083 34.5728]	43.04	45.97	0.94	573	707	0.81
121	[26.8182 28.9862]	30.20	32.52	0.93	391	506	0.77
122	[24.6780 26.8776]	28.26	31.46	0.90	323	441	0.73
123	[30.9756 30.0575]	41.53	44.39	0.94	540	696	0.78
124	[27.1126 26.4202]	36.38	39.19	0.93	452	595	0.76
125	[28.8287 31.9895]	37.88	40.57	0.93	423	572	0.74
126	[28.7190 29.6436]	39.69	42.42	0.94	485	637	0.76
127	[34.0735 35.7289]	52.48	55.07	0.95	738	911	0.81
128	[49.2552 48.5583]	101.72	105.23	0.97	1355	1630	0.83
129	[28.8620 29.0341]	32.67	33.71	0.97	486	558	0.87
130	[24.2233 25.5744]	26.86	29.91	0.90	328	430	0.76
131	[26.7575 26.7166]	28.83	30.80	0.94	305	367	0.83
132	[49.0196 50.0018]	95.82	98.34	0.97	1336	1633	0.82
133	[44.9721 46.1867]	77.61	80.25	0.97	1048	1291	0.81
134	[24.4473 25.2998]	26.70	29.15	0.92	314	427	0.74
135	[38.0431 37.4602]	76.87	79.66	0.96	1095	1369	0.80
136	[29.8402 30.3018]	40.66	43.68	0.93	513	676	0.76
137	[27.8104 26.3476]	30.15	33.40	0.90	388	538	0.72
138	[37.5534 36.7115]	53.98	56.47	0.96	784	974	0.80
139	[29.4125 29.4471]	35.78	38.62	0.93	439	577	0.76
140	[37.9663 41.4970]	56.52	60.13	0.94	808	1010	0.80
141	[31.9151 32.1610]	48.85	51.65	0.95	734	907	0.81
142	[29.8893 33.3280]	47.25	50.18	0.94	560	750	0.75
143	[34.2745 34.8544]	47.62	50.12	0.95	695	838	0.83
144	[23.1959 21.2188]	24.23	26.69	0.91	297	393	0.76
145	[28.4099 28.2990]	33.83	36.77	0.92	395	505	0.78
146	[37.9007 37.1634]	70.64	72.18	0.98	934	1138	0.82
147	[27.6728 28.7461]	39.42	42.46	0.93	563	709	0.79
148	[32.9863 33.3576]	47.82	51.39	0.93	680	878	0.77
149	[45.1331 47.9658]	96.23	98.70	0.97	1509	1841	0.82
150	[44.6013 46.1590]	99.83	102.40	0.97	1353	1673	0.81
151	[40.3806 40.0726]	65.11	68.47	0.95	936	1185	0.79
152	[36.4048 37.7172]	66.41	69.70	0.95	847	1082	0.78
153	[26.9165 27.8819]	33.96	37.04	0.92	353	491	0.72
154	[36.2332 38.1856]	49.21	50.97	0.97	614	776	0.79
155	[37.9760 40.2984]	52.81	55.94	0.94	723	915	0.79
156	[32.4807 32.1120]	48.03	51.23	0.94	655	830	0.79
157	[29.1994 29.7479]	44.08	47.34	0.93	524	702	0.75
158	[32.3910 31.2398]	44.64	47.42	0.94	579	734	0.79
159	[39.2953 40.4273]	67.47	70.08	0.96	1100	1341	0.82
160	[28.3400 29.5595]	36.00	38.92	0.93	447	597	0.75
161	[26.8033 27.8358]	36.23	38.66	0.94	487	615	0.79
162	[29.9692 31.3720]	39.70	42.33	0.94	562	715	0.79
163	[36.7026 36.2058]	50.97	54.23	0.94	770	938	0.82
164	[27.5185 30.4537]	38.04	40.77	0.93	514	648	0.79
165	[27.1416 30.1631]	43.65	47.06	0.93	526	699	0.75
166	[38.7249 38.6721]	68.35	71.18	0.96	929	1156	0.80
167	[33.5261 32.9187]	48.12	51.43	0.94	686	861	0.80
168	[34.4943 35.7830]	49.25	51.36	0.96	713	880	0.81
169	[36.0201 36.0469]	47.46	50.68	0.94	741	896	0.83
170	[33.2642 34.2105]	46.32	49.27	0.94	782	950	0.82
171	[33.1478 34.0192]	52.99	56.23	0.94	782	988	0.79
172	[38.5844 40.0740]	61.43	64.44	0.95	1001	1203	0.83

Table 1: Continue

No.	Boundary mapped image centroid	Original image major axis diameter (pixels)	Boundary mapped image major axis diameter (pixels)	Ratio (original dia./ boundary dia)	Original image area (square pixels)	Boundary mapped image area (square pixels)	Ratio (original area/ boundary mapped image area)
173	[41.0865 38.6391]	77.83	80.28	0.97	1283	1538	0.83
174	[27.8423 30.0590]	40.12	43.10	0.93	612	780	0.78
175	[25.1124 23.9672]	27.71	30.77	0.90	306	427	0.72
176	[34.1137 33.7388]	47.49	50.23	0.95	645	827	0.78
177	[28.5720 30.2798]	40.85	43.51	0.94	580	729	0.80
178	[38.9898 38.5098]	58.12	60.89	0.95	867	1075	0.81
179	[27.7940 28.7116]	38.13	41.66	0.92	543	704	0.77
180	[42.8485 42.5401]	72.13	74.18	0.97	1096	1333	0.82
181	[26.3890 27.6057]	30.13	33.21	0.91	425	563	0.75
182	[30.5536 30.5975]	40.36	43.82	0.92	600	728	0.82
183	[25.0335 27.3046]	32.46	34.87	0.93	449	568	0.79
184	[28.1566 28.5081]	38.04	40.03	0.95	534	677	0.79
185	[34.2880 35.5287]	51.57	54.17	0.95	692	889	0.78
186	[25.0973 26.3641]	26.19	29.43	0.89	280	401	0.70
187	[27.9626 27.7683]	37.80	41.03	0.92	509	669	0.76
188	[31.5365 32.4071]	53.24	55.13	0.97	802	958	0.84
189	[37.4121 36.4187]	55.98	59.13	0.95	859	1058	0.81
190	[40.2592 38.6232]	61.07	63.59	0.96	981	1173	0.84
191	[25.6935 25.6525]	33.13	35.71	0.93	520	659	0.79
192	[25.3663 25.4066]	30.36	33.47	0.91	404	546	0.74
193	[30.2041 31.5176]	43.37	45.78	0.95	689	823	0.84
194	[30.0319 29.8300]	38.34	41.25	0.93	503	659	0.76
195	[37.2248 38.6959]	69.67	72.64	0.96	962	1210	0.80
196	[25.4519 27.3267]	33.39	35.51	0.94	445	551	0.81
197	[29.8671 29.1329]	39.06	42.15	0.93	503	662	0.76
198	[36.0437 34.6972]	54.71	57.68	0.95	780	984	0.79
199	[32.4070 32.5327]	40.47	43.68	0.93	644	796	0.81
200	[35.1640 36.5299]	47.95	50.76	0.94	744	921	0.81
201	[36.7601 38.3270]	62.86	66.28	0.95	1118	1367	0.82
202	[26.5181 27.4267]	34.06	37.31	0.91	538	689	0.78
203	[34.5226 34.7350]	50.44	53.61	0.94	892	1083	0.82
204	[31.3282 31.5067]	47.42	50.46	0.94	858	1042	0.82
205	[39.7481 38.5613]	60.56	63.73	0.95	1100	1338	0.82
206	[35.2632 33.7197]	59.17	62.03	0.95	1054	1288	0.82
207	[23.3516 24.1728]	27.12	30.11	0.90	368	492	0.75
208	[32.9188 34.4385]	46.73	50.08	0.93	765	960	0.80
209	[29.7746 30.7815]	35.83	39.48	0.91	577	723	0.80
210	[40.2170 39.7674]	59.94	63.31	0.95	1074	1281	0.84
211	[32.4565 32.6325]	47.55	50.45	0.94	772	955	0.81
212	[32.4680 33.8709]	46.88	50.21	0.93	784	968	0.81
213	[27.5585 30.1582]	34.25	37.75	0.91	596	752	0.79
214	[36.3020 39.5470]	57.47	60.19	0.95	942	1139	0.83
215	[37.4459 36.8153]	62.94	65.91	0.95	1157	1386	0.83
216	[30.4647 29.8111]	37.56	40.93	0.92	652	794	0.82
217	[25.9044 28.3244]	36.85	40.36	0.91	581	743	0.78
218	[31.9364 34.2611]	45.16	48.96	0.92	732	927	0.79
219	[33.3135 36.2791]	55.00	58.51	0.94	1085	1308	0.83
220	[27.8819 30.6750]	40.57	42.88	0.95	786	957	0.82
221	[39.5110 42.3905]	71.22	74.64	0.95	1385	1634	0.85
222	[40.2030 38.7034]	56.03	59.58	0.94	1183	1399	0.85
223	[44.5525 44.6775]	72.06	75.44	0.96	1135	1352	0.84
224	[48.0502 49.5722]	83.95	86.50	0.97	1472	1753	0.84
225	[36.0557 39.3780]	59.98	62.71	0.96	928	1148	0.81
226	[29.7716 29.9290]	38.03	40.56	0.94	518	648	0.80
227	[31.5687 30.4835]	39.14	42.51	0.92	618	786	0.79
228	[35.5343 34.0741]	51.23	54.45	0.94	1070	1282	0.83
229	[46.5807 43.2889]	91.18	93.20	0.98	1529	1779	0.86
230	[52.8356 53.6145]	111.10	113.46	0.98	1833	2166	0.85
231	[45.6916 44.1420]	81.51	83.80	0.97	1463	1725	0.85
232	[24.3987 24.5850]	26.72	30.20	0.88	489	612	0.80
233	[33.2636 33.8503]	47.14	49.86	0.95	748	922	0.81
234	[34.4428 37.0790]	50.31	53.92	0.93	1101	1303	0.84
235	[30.6392 32.7028]	41.38	44.30	0.93	857	1006	0.85
236	[37.3179 39.2879]	59.30	61.37	0.97	1435	1667	0.86

Table 1: Continue

No.	Boundary mapped image centroid	Original image major axis diameter (pixels)	Boundary mapped image major axis diameter (pixels)	Ratio (original dia./ boundary dia)	Original image area (square pixels)	Boundary mapped image area (square pixels)	Ratio (original area/ boundary mapped image area)
237	[28.1318 27.3162]	33.94	36.80	0.92	628	759	0.83
238	[31.6159 33.4450]	40.53	43.90	0.92	749	919	0.82
239	[56.9826 57.3785]	129.75	131.81	0.98	2495	2869	0.87
240	[39.2884 41.8575]	76.11	78.58	0.97	1523	1782	0.85
241	[30.7373 30.6448]	38.25	40.37	0.95	545	670	0.81
242	[30.1667 32.0805]	41.02	43.79	0.94	906	1068	0.85
243	[32.3287 34.1614]	41.26	45.19	0.91	828	1010	0.82
244	[39.7588 38.3101]	58.07	60.73	0.96	961	1103	0.87
245	[29.9227 28.9430]	36.75	39.07	0.94	618	737	0.84
246	[47.4137 45.3505]	91.05	93.37	0.98	1379	1552	0.89
247	[31.4011 32.1053]	43.07	44.31	0.97	616	703	0.88
248	[43.1486 39.9778]	76.89	76.70	1.00	1198	1353	0.89
249	[41.8287 42.2792]	71.67	74.32	0.96	1044	1214	0.86
250	[37.8606 41.9242]	61.74	64.58	0.96	1072	1227	0.87
251	[30.8228 29.4850]	42.84	44.88	0.95	749	903	0.83
252	[56.5689 53.7292]	125.00	126.07	0.99	2546	3050	0.83
253	[28.0887 29.5734]	36.31	38.18	0.95	479	586	0.82
254	[36.5931 37.6571]	52.43	54.69	0.96	997	1155	0.86
255	[37.5476 38.1569]	71.61	74.25	0.96	1337	1574	0.85
256	[39.1482 39.5593]	63.83	67.02	0.95	1060	1289	0.82
257	[37.5100 38.6694]	65.34	67.51	0.97	1366	1606	0.85
258	[31.0362 31.1853]	44.83	47.54	0.94	734	912	0.80
259	[29.4730 29.9564]	38.96	42.12	0.93	904	1055	0.86
260	[43.9274 47.5520]	77.91	80.86	0.96	1588	1886	0.84
261	[61.1146 65.4826]	127.75	131.04	0.97	2718	3158	0.86
262	[33.4525 35.2926]	48.62	52.07	0.93	828	1032	0.80
263	[30.4807 29.8072]	39.60	42.21	0.94	585	726	0.81
264	[37.4498 40.3227]	62.82	65.71	0.96	1148	1354	0.85
265	[38.4346 38.8584]	58.32	61.77	0.94	1013	1215	0.83
266	[51.6145 48.9165]	96.14	98.80	0.97	1729	2000	0.86
267	[33.2142 33.3221]	44.56	47.01	0.95	930	1102	0.84
268	[34.6961 34.9899]	46.99	49.87	0.94	729	895	0.81
269	[34.2481 37.0077]	49.13	50.01	0.98	925	1036	0.89
270	[27.3137 27.9644]	39.31	42.34	0.93	755	899	0.84
271	[33.8047 38.8823]	52.09	53.20	0.98	959	1096	0.88
272	[35.3965 36.6104]	59.30	61.56	0.96	1129	1314	0.86
273	[37.6492 35.8454]	60.61	61.53	0.99	1221	1371	0.89
274	[34.6788 33.3166]	52.46	56.05	0.94	1174	1314	0.89
275	[25.6995 26.1541]	33.86	35.38	0.96	565	649	0.87
276	[29.9294 29.3195]	42.58	44.19	0.96	778	892	0.87
277	[27.7161 28.3427]	33.20	34.55	0.96	347	391	0.89
278	[30.6893 31.3000]	45.75	48.88	0.94	666	840	0.79
279	[24.2059 24.7347]	32.68	34.24	0.95	408	505	0.81
280	[26.0678 27.5904]	37.06	38.83	0.95	519	664	0.78
281	[26.0935 26.3819]	37.38	38.60	0.97	560	631	0.89
282	[28.2795 29.9154]	44.66	46.85	0.95	560	662	0.85
283	[23.2284 24.2513]	27.79	27.91	1.00	341	394	0.87
284	[28.6888 28.8262]	45.62	48.31	0.94	549	633	0.87
285	[23.5414 23.9499]	29.15	30.67	0.95	435	519	0.84
286	[33.8658 32.5973]	55.47	56.49	0.98	751	894	0.84
287	[26.8383 27.7632]	36.30	38.38	0.95	433	532	0.81
288	[26.7254 26.9905]	38.30	40.87	0.94	495	630	0.79
289	[30.7921 27.8247]	41.15	42.97	0.96	476	582	0.82
290	[24.1028 22.7056]	28.05	30.24	0.93	333	428	0.78
291	[29.0852 29.3322]	40.97	44.14	0.93	461	587	0.79
292	[29.7322 27.6868]	42.13	43.50	0.97	559	661	0.85
293	[33.3831 32.7469]	55.34	56.39	0.98	754	885	0.85
294	[39.0349 39.0563]	63.71	66.23	0.96	877	1031	0.85
295	[23.9008 24.9534]	31.93	34.08	0.94	381	494	0.77
296	[23.6303 24.1534]	33.23	35.00	0.95	366	476	0.77
297	[34.7083 35.2707]	50.95	54.34	0.94	585	713	0.82
298	[27.8626 27.6209]	38.00	40.04	0.95	445	546	0.82
299	[34.1548 33.9588]	47.39	48.48	0.98	609	704	0.87
300	[24.1526 23.3709]	31.06	33.15	0.94	355	426	0.83

Table 1: Continue

No.	Boundary mapped image centroid	Original image major axis diameter (pixels)	Boundary mapped image major axis diameter (pixels)	Ratio (original dia./ boundary dia)	Original image area (square pixels)	Boundary mapped image area (square pixels)	Ratio (original area/ boundary mapped image area)
301	[28.6497 27.8567]	44.49	47.06	0.95	492	628	0.78
302	[38.3790 38.5131]	71.57	73.79	0.97	925	1103	0.84
303	[36.3878 36.6809]	68.23	70.92	0.96	1041	1266	0.82
304	[34.6230 34.7311]	64.86	67.60	0.96	937	1138	0.82
305	[42.0403 43.1346]	88.98	91.80	0.97	1305	1612	0.81
306	[29.4662 30.7488]	45.81	48.21	0.95	654	800	0.82
307	[36.0799 36.4494]	69.37	72.50	0.96	1004	1226	0.82
308	[33.4187 32.4261]	49.49	51.48	0.96	1127	1366	0.83
309	[31.8892 30.3500]	47.32	48.83	0.97	621	740	0.84
310	[34.3630 34.2814]	63.27	65.37	0.97	919	1091	0.84
311	[36.1257 36.2144]	64.37	67.65	0.95	957	1138	0.84
312	[33.9338 33.3118]	53.62	54.97	0.98	1021	1193	0.86
313	[50.0328 50.5630]	115.03	116.94	0.98	1420	1707	0.83
314	[33.7135 35.0951]	59.98	63.06	0.95	755	904	0.84
315	[31.3773 32.3997]	54.30	56.00	0.97	628	758	0.83
316	[28.4803 27.3890]	42.10	45.23	0.93	469	635	0.74
317	[32.9125 33.3280]	47.84	49.68	0.96	849	994	0.85
318	[25.8264 26.5364]	38.99	40.67	0.96	535	645	0.83
			std dev	0.02			0.04
			Mean	0.95			0.81

of the boundary mapped image, when multiplied with its respective mean (from table) will surely approximate the length or area of its corresponding original image within 5% tolerance. If suitable training algorithms like neural networks or fuzzy algorithms are utilized (that are already in use, description of which is beyond the scope of this work), the length and area of the original images can be obtained from the observations on boundary mapped images.

The Centroid of the boundary mapped image serves to identify the centre point of the boundary mapped chromosome image. Accompanied with suitable centromere segmentations algorithms (that are already in use, description of which is beyond the scope of this work), information about the exact location of the Centroid in the boundary mapped chromosome image can be extracted.

Hence, from this information, the chromosomes can be classified into Groups A to G (for autosomes) or into 22 pairs of chromosomes and the sex chromosomes (X and Y) or into X and Y chromosomes as per prevalent cytogenetic guidelines for chromosome identification.

Thus, we find that the DCT based GVF active contours which was used for chromosome image segmentation has got good potential for application as a tool for chromosome classification using the same observations generated during the segmentation process. Therefore, the DCT based GVF active contours can also serve as a tool for chromosome classification.

CONCLUSIONS

The discussion yields valuable insight into the capabilities of DCT based GVF active contours, hitherto employed as an efficient chromosome segmentation tool to extend as a suitable chromosome classification tool. Hence, the DCT based GVF active contours can be used as a suitable chromosome classification tool.

ACKNOWLEDGMENTS

The authors extend their heartfelt thanks to Dr. Michael Difilippantonio, Staff Scientist at the Section of Cancer Genomics, Genetics Branch/CCR/NCI/NIH, Bethesda MD; Prof. Ekaterina Detcheva at the Artificial Intelligence Department, Institute of Mathematics and Informatics, Sofia, Bulgaria; Prof.Ken Castleman and Prof.Qiang Wu, from Advanced Digital Imaging Research, Texas and Wisconsin State Laboratory of Hygiene--<http://worms.zoology.wisc.edu/zooweb/Phelps/karyotype.html for their help in providing chromosome spread images.

REFERENCES

<http://www.colorado.edu/MCDB/MCDB2150Fall/notes00/L0001.html>
<http://home.earthlink.net/~heinabilene/karyotypes/karyoty.htm>

<http://arbl.cvmbs.colostate.edu/hbooks/genetics/medgen/chromo/chromosomes.html>

Britto, A.P. and G. Ravindran, 2005. Boundary mapping of chromosome images using gradient vector flow active contours and investigations, Acad. Open Internet J., <http://www. acadjournal.com/2005/ v15/ part6/p6/>

Britto, A.P. and G. Ravindran, 2005. Comparison of boundary mapping efficiency of gradient vector flow active contours and their variants on chromosome spread images. J. Applied Sci., 5: 1452-1460.

Britto, A.P. and G. Ravindran, 2005. Boundary mapping of chromosome spread images using optimal set of parameter values in discrete cosine transform based gradient vector flow active contours. J. Applied Sci. (accepted, in print).

Britto, A.P. and G. Ravindran, 2005. Evaluation of standardization of curve evolution based boundary mapping technique for chromosome spread images. Inform. Technol. J. (accepted, in print).

Kass, M., A. Witkin and D. Terzopoulos, 1987. Snakes: Active contour models, Intl. J. Comp. Vision 1: 321-331.

Tang, J. and S.T. Acton, 2004. A DCT based gradient vector flow snake for object boundary detection. 6th IEEE Southwest Symposium on Image Analysis and Interpretation, pp: 157-161.

Xu, C. and J.L. Prince, 1998. Snakes, shapes and gradient vector flow, IEEE Transactions on Image Process, 7: 359-369.

Xu, C. and J.L. Prince, 2000. Gradient vector flow deformable models. Handbook of Medical Imaging, Academic Press, pp: 159-169.